

# Chaotic Mixing in Two- And Three-Dimensional Cavity Flows

Thuy Hong Van-Le\*, Sangmo Kang, Yong Kweon Suh

Department of Mechanical Engineering

Dong-A University

840 Hadan-2 dong, Saha-gu, Busan, 604-714

REPUBLIC OF KOREA

**Abstract:** The aim of this article is to examine the properties and qualities of chaotic mixing by considering a two- and three-dimensional cavity flows. Finite volume method is employed to obtain accurate descriptions of the velocity field which form the basis for mixing analysis. Furthermore, we also got the mixing efficiency using Poincaré section and Lyapunov exponent. In the present study, the primary form of chaotic mixing is generated by using time-periodic electro-osmotic flow, driven by an electric field. The surface zeta-potential causes different flow fields which are susceptible to chaotic advection and mixing. Depending on the above properties, a non-uniform slip-velocity is produced by imposing four non-uniform zeta-potential surfaces to the bottom wall during first half of the period and to the top wall during second half of the period, respectively. The various parameters involved in this study are the Peclet number and the modulation period. The effect of these parameters on the flow patterns within the cavity is investigated numerically. There is also an important value of mixing index which describes the quality of mixing, is also obtained.

**Key-Words:** Chaotic Mixing, Mixing Index, Poincaré section and Lyapunov exponent.

## 1. Introduction

There has been a recently developing surge of fundamental properties of the mixing due to its application in manufacturing, food, pharmacology and other industries. Some researchers are successfully studied on electro-osmotic flows in the non-uniform zeta-potentials such as Qian and Bau [13], Ajdari [14], H. Aref [15] and etc. Understanding of this article can help to create a good mixing in cavity flow by switching the various flow fields which are caused by imposing the non-uniform zeta-potential surfaces to the walls of cavity.

## 2. Problem Formulation and Analytical Solution

### 2.1 Two-dimensional cavity flow

We have considered the unsteady two-dimensional motion of an incompressible fluid within a closed square cavity where four electrodes are attached to the bottom and top walls of it as shown in Figure 1. This generates the relevant electro-osmotic slip velocity at the walls.

The governing equations for this problem are written in a dimensionless form as follows

$$\nabla \cdot \mathbf{u} = 0, \quad (1)$$

$$\frac{\partial \mathbf{u}}{\partial t} + \mathbf{u} \cdot \nabla \mathbf{u} = -\nabla p + \frac{1}{\text{Re}} \nabla^2 \mathbf{u}, \quad (2)$$

$$\frac{\partial C}{\partial t} + \mathbf{u} \cdot \nabla C = \frac{1}{\text{Pe}} \nabla^2 C \quad (3)$$

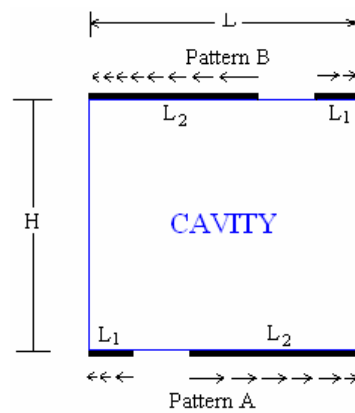


Fig.1 2-D Geometry of the cavity and the periodic non-uniform boundary conditions at the top and the bottom walls.

$$L_1 = 0.2L, L_2 = 0.6L$$

Pattern A and B corresponds with the flow fields applied to bottom wall during the first half of the period and to top wall during the second half of the period, respectively.

where  $C$  is the concentration,  $Re(=UL/\nu)$  is the Reynolds number and  $Pe(=UL/D)$  is the Peclet number.  $L$  is the characteristic length,  $U$  is the characteristic velocity,  $D$  is the concentration diffusivity,  $\nu$  is the kinematic viscosity and  $t$  is the dimensionless time.

The boundary conditions for velocity field and concentration are:

At the side walls:

- Velocities: No-slip condition  $u = v = 0$
- Concentration: zero-gradient condition  $\frac{\partial C}{\partial x} = 0$

At the top and bottom walls:

- Velocities: No-slip condition  $v = 0$
- Concentration: zero-gradient condition  $\frac{\partial C}{\partial y} = 0$

At the bottom wall:

- During first half period  $0 \leq t < T/2$

$$ub_1 = -\frac{3.33}{2L}x \text{ for } 0 \leq x \leq 0.2 \quad (4)$$

$$ub_2 = \frac{1}{(0.4L-1)}(x-1) \text{ for } 0.4 \leq x \leq 1 \quad (5)$$

where  $T$  is modulation period.

- During second half period  $T/2 \leq t \leq T$

$$ut_1 = -\frac{5}{3L}x \text{ for } 0 \leq x \leq 0.6 \quad (6)$$

$$ut_2 = -\frac{0.333}{(0.8L-1)}(x-1) \text{ for } 0.8 \leq x \leq 1 \quad (7)$$

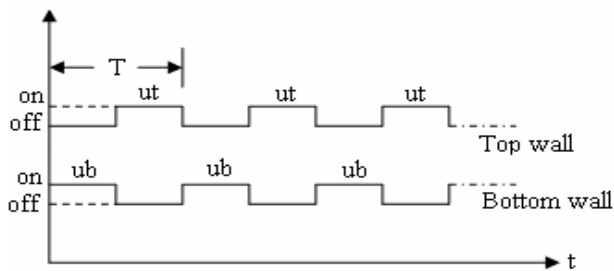


Fig.2 The non-uniform boundary conditions for  $u$ -velocity at the top and bottom walls.

In this case, we used the non-uniform staggered grid system, obtained by transformation from the Castien coordinates  $(x, y)$  to the new coordinates  $(\xi, \eta)$  as follows:

$$\xi = \frac{1}{2} \left[ 1 + \frac{\sinh[b(x-1/2)]}{\sinh[b/2]} \right] \quad (8)$$

$$\eta = \frac{1}{2} \left[ 1 + \frac{\sinh[b(y-1/2)]}{\sinh[b/2]} \right] \quad (9)$$

The governing equations are discretized in time using finite volume method. The Explicit Euler method is used for integration of momentum and concentration equations in time.

- For  $x$  and  $y$  momentum equations:

$$u_{i,j}^n = u_{i,j}^{n-1} - \frac{\Delta t}{\Delta x_e} (P_{i+1,j} - P_{i,j}) + \Delta t \cdot f_{i,j}^{n-1} \quad (10)$$

$$v_{i,j}^n = v_{i,j}^{n-1} - \frac{\Delta t}{\Delta y_n} (P_{i,j+1} - P_{i,j}) + \Delta t \cdot g_{i,j}^{n-1} \quad (11)$$

The convection and diffusion terms combined in 'f' and 'g'.

- For concentration equation

$$C_{i,j}^n = u_{i,j}^{n-1} - \Delta t \cdot h_{i,j}^{n-1} \quad (12)$$

Mixing index is defined by the following equation

$$D = \sqrt{\frac{1}{N} \sum_{i,j} (1 - C_{i,j} / \bar{C})^2} \quad (13)$$

Where  $C_{i,j}$ : concentration at position  $(i,j)$  in the computational domain;  $\bar{C}$ : the average concentration.  $N$ : is the total number of nodes.

## 2.2 Three-dimensional cavity flow

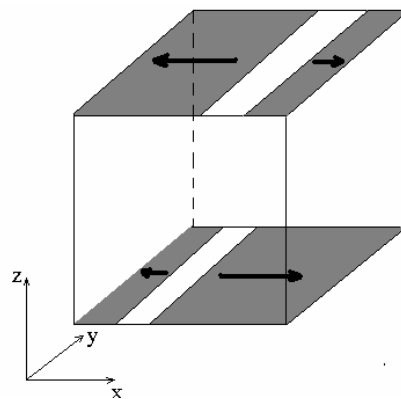


Fig.3 3-D Geometry of the cavity

The governing equation for this case is same as given in section 2.1 but  $u = (u,v,w)^T$ . Also the fluid properties inside cavity do not change. The zeta-potential is applied to the surfaces as shown in Figure 3 where it is applied to walls in 2-D case. The 3-D code will be developed using the FVM method.

### 2.3 Mixing effect using Poincaré section and Lyapunov exponent

• Poincaré section is a graphical analysis tool to capture interesting features such as mixing zones in cavity flow. Otherwise, it is also a surface in the phase space that cuts across the flow of a given system. With a 2D cavity flow, the positions of a point in calculation domain are advanced by 4<sup>th</sup> Runge-Kutta method as follows:

$$\frac{dx}{dt} = u; \quad \frac{dy}{dt} = v \quad (17)$$

$$x^n = x^0 + [K_{1x} + 2(K_{2x} + K_{3x}) + K_{4x}]/6 \quad (18)$$

$$y^n = y^0 + [K_{1y} + 2(K_{2y} + K_{3y}) + K_{4y}]/6 \quad (19)$$

Where  $K_{1x}, K_{1y}, \dots, K_{4y}$  is the coefficients of Runge-Kutta.

• Lyapunov exponent describes chaotic mixing by determining the position of two initially nearby particles will be extremely different after a certain time.

The best mixing effect will be obtained when Lyapunov exponent approaches to a maximum value. The largest Lyapunov coefficient should be positive in the chaotic state, when the Lyapunov exponent is defined as:

$$\lambda = \frac{1}{T} \ln \left( \frac{L_i}{d_0} \right); \quad i = 1 \rightarrow N \quad (19)$$

$$L_i = \left[ (x_{i+1} - x_i)^2 + (y_{i+1} - y_i)^2 \right]$$

Where T is modulation period,  $L_i$  is distance between two particles at the specified time step and  $d_0$  is distance between the two initial particles.

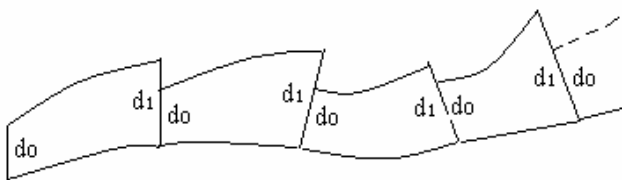


Fig. 4 Schematic for calculation for calculating the Lyapunov exponent.

We choose arbitrary two initial points to track the path of the main particle and to calculate the Lyapunov exponent in the mixing zone. The distance between the two particles should be less than the initial distance  $d_0$ .

## 3. Results and Discussion

### 3.1 Results for 2D case

The FORTRAN code has been developed for the 2D case which gave us quite good results. The numerical solutions were obtained for the grid 101x101, which was selected by grid convergence test and for the fixed Reynolds number  $Re = 10$ . The mixing process is attained steady state in whole domain of cavity after total time steps  $Nsteps = 500,000$  for  $Pe = 2000$  and  $Nsteps = 600,000$  for  $Pe = 10,000$ . In each case, the results are obtained for the five values of modulation periods 1, 5, 10, 15 and 20.

Mixing performance is obtained from solving concentration equation correspond with various initial conditions of concentration distribution. The Poincaré section and Lyapunov exponent are employed to get mixing index for various boundary conditions of streamline velocity.

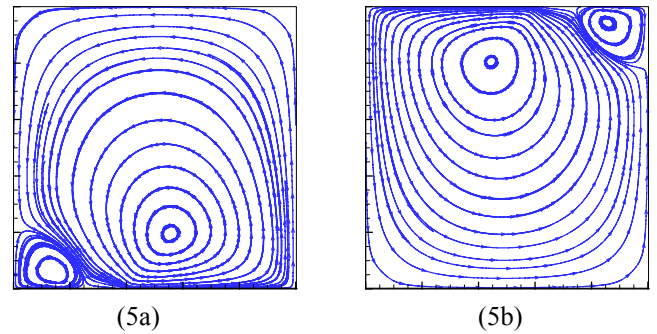


Fig.5 Streamlines pattern for the cavity flow at steady state corresponding to  $T=1$ , (a) first half period and (b) second half period.

With above boundary conditions, we got the velocity field which is symmetric for every half period. The streamlines appear four eddies, two at the bottom wall during first half period and remaining two at the top wall during second half period.

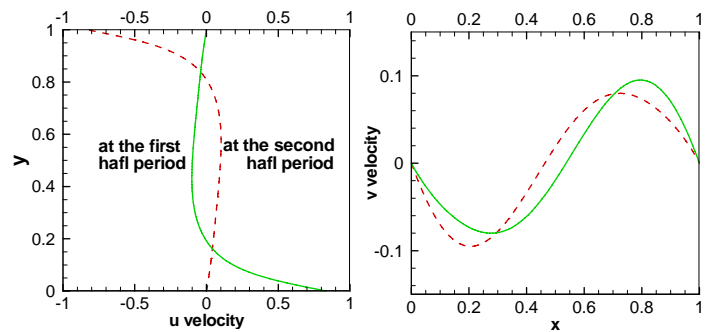


Fig. 6 Steady state u and v velocities along the vertical and horizontal center line of cavity.

The grid convergence test has been carried out considering 51x51, 101x101 and 201x201 grid systems. The following graph gives the details of the test. It found that 101x101 grid system is suitable for our case.

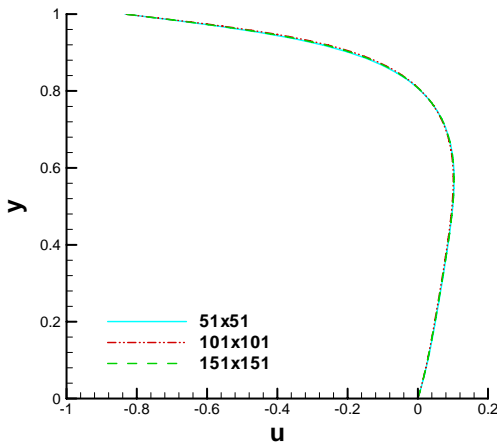


Fig. 7 Grid convergence test.

### 3.1 Mixing effect with respect to various initial conditions of concentration distribution

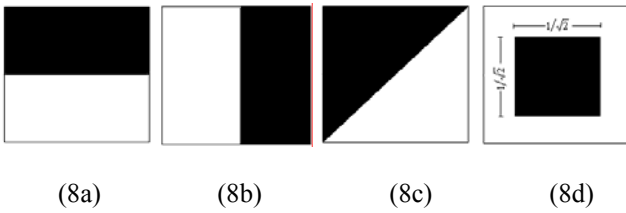


Fig.8 Concentration distribution conditions used in the simulation;  $C = 1$  for black and  $C = 0$  for white. (a) HS – horizontal separation; (b) VS – vertical separation; (c) DS – diagonal separation and (d) SS – square separation

The results show that, for the small Peclet number ( $Pe = 2000$ ), the change in mixing pattern is negligible with varying modulation periods (1 to 20) at a specified time step. However, when we increase the Peclet number ( $Pe = 10000$ ) the mixing pattern is rather different with respect to different modulation periods. Especially, with the higher value of modulation, the more early mixing process is obtained at a specified Peclet number. Furthermore, we know that the small Peclet number causes a high diffusion, so the mixing process quicker for low Peclet numbers than the higher Peclet numbers.

The best mixing index are collected for every initial condition at  $Pe = 2000$  and  $Pe = 10000$  (Figures. 10 and 11). We found that mixing effect is specifically affected by the initial condition of C-distribution. Among these

results, the best mixing effect is achieved in case of HS ( $Pe = 2000$ ) and DS in case of  $Pe = 10000$ .

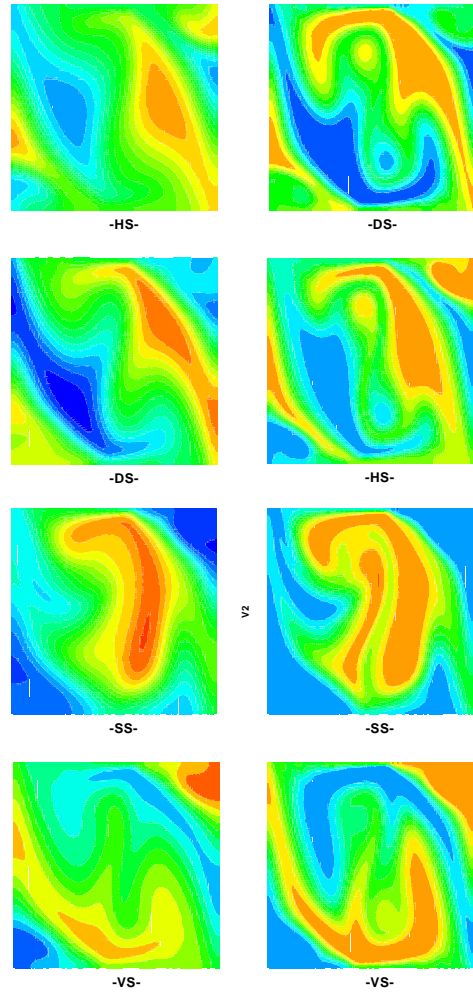


Fig.9 Mixing effect with respect to various initial conditions of concentration distribution at  $t = 20$  (RHS- results for  $Pe = 2000$ ; LHS- results for  $Pe = 10000$ )

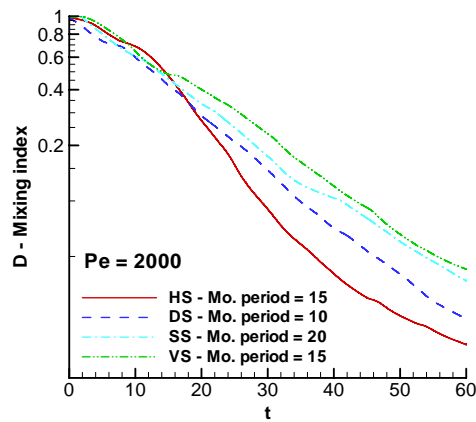


Fig. 10 Variation of Mixing index with respect to dimensionless time for  $Pe = 2000$ .

For  $Pe = 2000$ , the mixing is better compared with  $Pe = 10000$ . That means at low  $Pe$  number, diffusion is

more, so many thin layers will be observed in flow pattern.

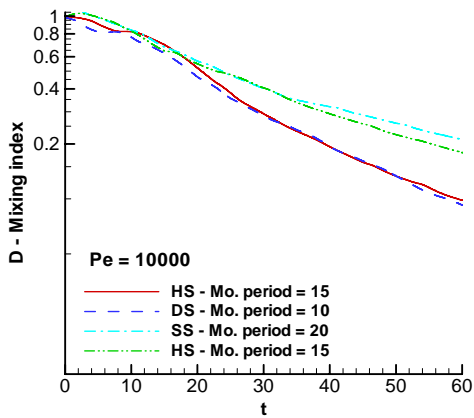


Fig. 11 Variation of Mixing index with respect to dimensionless time for  $Pe = 10000$ .

### 3.2 Results for Poincaré section and Lyapunov exponent

We will capture the particle's trajectory by calculating the equation of positions. The 1025 started points are distributed uniformly in cavity domain.

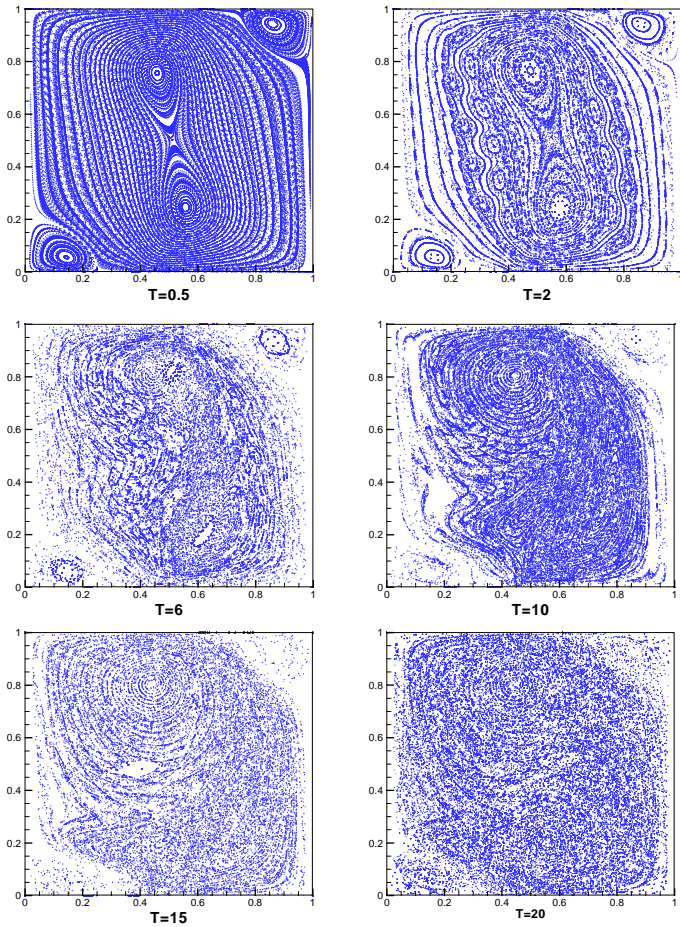


Fig.12 Poincaré section with respect to various modulation periods.

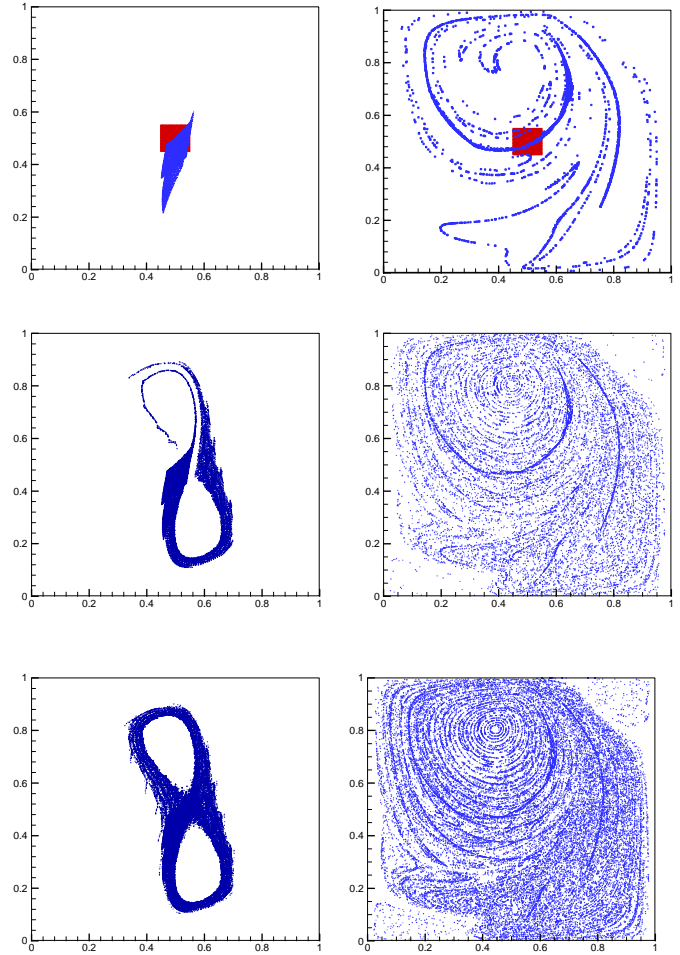


Fig. 13 The deformation of a material of edge size 0.1 initially ( $t = 0$ ) centred at  $(0.45, 0.45)$ .

We can see the mixing effect is better gradually when we increase the modulation period. At the smallest modulation period, the trajectory of the particle is clear as streamlines in chaotic and regular domains. But when modulation period increases the particles are distributed uniformly in whole domain of cavity. Therefore, we can get best mixing effect when we input the enough high value of modulation period. The deformation of blob is also considered with respect to various values of modulation periods. After two periods, the square blob has already turned into thin line. When the modulation period is relatively small, the blob stretches, deforms and elongates slowly. At  $T = 2$ , all particles just wandered around the small fixed zone after 20 periods. The blob is deformed fully and the fluid particles spread to cover almost the entire cavity domain with respect to  $T = 20$ .

Furthermore, when we impose zeta-potential surfaces to another wall which means we change boundary condition at the walls of cavity; we also get the rather different mixing effects.

Appropriate to different flow patterns (shown in Fig. 12), we computed the Lyapunov exponent for various time periods.

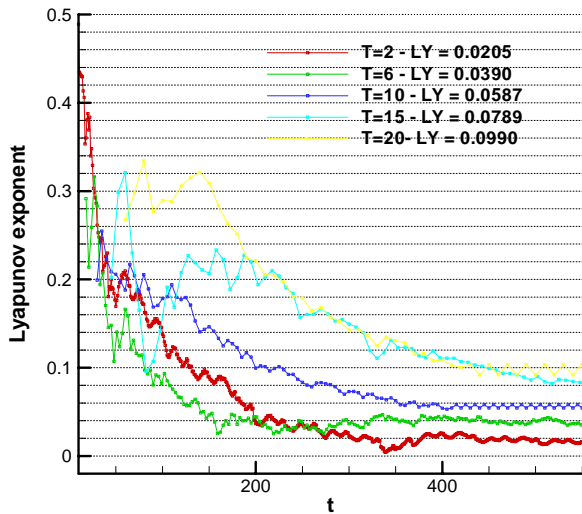


Fig.14 Lyapunov exponent at various modulation periods.

The above results were obtained by choosing the two initial points  $(0.5, 0.4)$  and  $(0.5, 0.4-D_0)$  where  $D_0 = 10^{-7}$ . Lyapunov exponent is largest ( $LE = 0.099$ ) with respect to value of modulation period  $T= 20$ . These results matched with which obtained in previous section correspond with solving the concentration equation.

### 3.2 Results for 3-D case

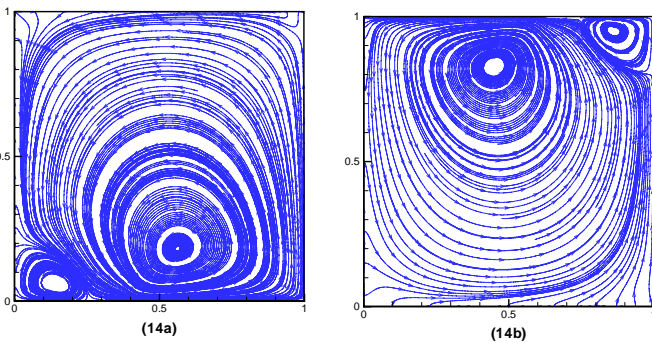


Fig. 14 Streamlines in plane  $(x,z)$  at  $y=1/2$  correspond to first half period (14a) and second half period (14b)

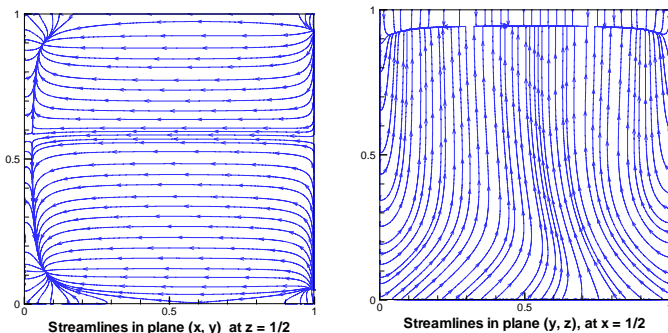


Fig. 15 Streamlines in plane  $(x,z)$  and  $(y, z)$

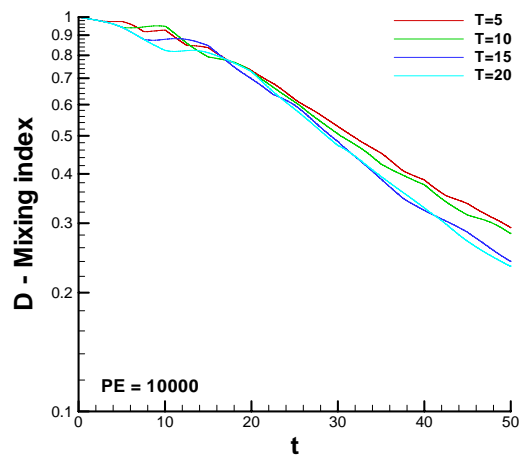
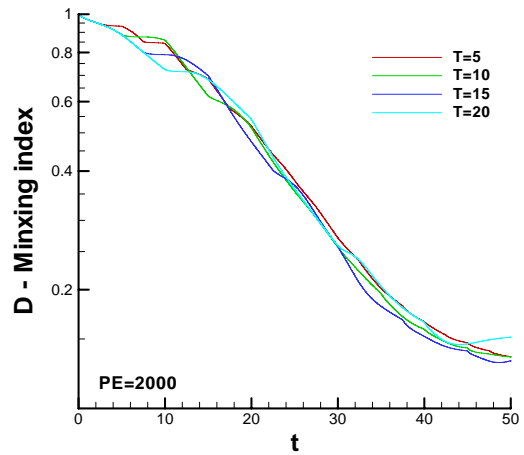


Fig.14 Variation of Mixing index with respect to dimensionless time for  $Pe= 2000$  (above) and for  $Pe= 10000$  (below).

Additional results for 3-D case will be implemented and presented in conference.

### 3. Conclusion

The primary aim of the present work paper was to develop the numerical code of finite element method for solving the chaotic mixing properties of flows generated by solid walls undergoing alternating boundary conditions periodically in every period at the top and bottom walls in a two dimensional cavity. The chaotic mixing is enough good depend on the modulation of the chosen period for imposing of the boundary conditions at the solid wall of cavity and the Peclet number.

The fairly good results of chaotic mixing in this case are to demonstrate FVM is also an advantageous method for simulation of mixing problems. The Poincaré section and Lyapunov exponent are also the good methods to obtain the mixing performance in this case.

## ACKNOWLEDGEMENT

This work was supported from the National Research Laboratory Program of the Korea Science and Engineering Foundation.

## REFERENCES

- [1] *J. H. Ferziger, M. Peric*: Computational Methods for Fluid Dynamics, Springer, 1996, pp.149-204
- [2] *Patrick D. Anderson, Olesksiy S. Galaktionov, Gerrit W.M. Peters, Frans N. van de Vosse, Han E.H. Meijer*: Chaotic fluid mixing in non-quasi-static time-periodic cavity flows, *Heat and Fluid Flow*, 21 (2000), pp. 176-185.
- [3] *S.Cerbelli, A. Adrover, F. Creta and M. Giona*: Foundations of laminar chaotic mixing and spectral theory of linear operators, *Chemical Engineering Science.*, 61(2006), p2754-2761.
- [4] *Tatsuo Nishimura and Koji Kunitsugu*: Fluid mixing and mass transfer in two-dimensional cavities with time-periodic lid velocity, *Int. J. Heat and Fluid Flow* 18, pp.497-506, 1997
- [5] *Patrick D. Anderson, Olesksiy S. Galaktionov, Gerrit W.M. Peters, Frans N. van de Vosse, Han E.H. Meijer*: Mixing of non-Newtonian fluids in time-periodic cavity flows, *J. Non-Newtonian Fluid Mech*, 93 (2000), pp. 265-286.
- [6] *Fredrik Carlsson, Mihir Sen, Lennart Lofdahl*: Fluid mixing induced by vibrating walls, *European Journal of Mechanics B/Fluids*, 24 (2005), pp. 366-378.
- [7] *O.S Galaktionow, V.V. Meleshko, G.W.M Peters, H.E.H Meijer*: Stokes flow in a rectangular cavity with a cylinder, *Fluid dynamics Research*, 24(1999), pp. 81-102.
- [8] *L.M. de la Cruz, E. Ramos*: Mixing with time dependent natural convection, *International Communications in Heat and Mass Transfer*, 33 (2006), pp.191-198.
- [9] *A. L de Bortoli*: Mixing and Chemical reacting flow simulations inside square cavities, *Applied Numerical Mathematics*, 47 (2003), pp. 295-303.
- [10] *T.S. Krasnopolskaya, V.V.Meleshko, G.W.M Peters, H.E.H Meijer* : Mixing in Stokes flow in an annular wedge cavity, *Eur. J. Mech. B/Fluids*, 18 (1999), pp. 793-822.
- [11] *C. Migeon, A. Texier and G. Pineau*: Effects of lid-driven cavity shape on the flow establishment phase, *Fluid and Structures*, (2000) 14, pp. 469-488.
- [12] *Yong Kweon Suh*, On the problem of using mixing index based on the Concentration distribution, pp. 796-805, 2006.
- [13] *Shizhi Qian, Haim H. Bau*, Theoretical Investigation of Electroosmotic Flows and Chaotic Stirring in Rectangular Cavities, *Applied Mathematical Modelling*, August 2005, pages 726,735.
- [14] *A. Ajdari*, Electroosmosis on Inhomogeneously Charged Surfaces, *Physical Review Letters*, 75(1995), 775-758.
- [15] *H. Aref*, Stirring by chaotic advection, *Journal of Fluid Mechanics*, 134(1984), 1-21.